Journal of Applied Organometallic Chemistry

2026, Volume 6, Issue 2

Original Article

Comprehensive Computational Exploration of Copper (II)–Benzimidazole Complexes as DNA Gyrase B Inhibitors: Integrated Molecular Modeling and Molecular Dynamics Approaches

Sajja Ravindra Babu[a] | Venkata Ramana Singamaneni[b] | Joel Mart E.[c,*] | Pericharla Venkata Narasimha Raju[d] | Phanindra Erukulla[e] | Ajay Manukonda[f] | Kanaka Durga Hanumanthu[g] | S. Prema[h,*]

[a]*Department of Pharmacology, Mallareddy Institute of Pharmaceutical Sciences, Mallareddy Vishwavidyapeeth (Deemed to be University), Secunderabad, 500100, Telangana, India*
[b]*Department of Analytical Research and Development, Cambrex, Charles City, Iowa- 50616, USA*
[c]*Department of Pharmacology, School of Pharmaceutical Sciences, Vels Institute of Science, Technology and Advanced Studies (VISTAS), Chennai-600117, Tamil Nadu, India*
[d]*Department of Regulatory Affairs, Hikma Pharmaceuticals USA Inc.,2 Esterbrook Lane, Cherry Hill, NJ 08003, USA*
[e]*Department of Regulatory Affairs, Ricon Pharma LLC, 100 Ford Rd, Suite #9, Denville, NJ 07834, USA*
[f]*Department of Regulatory Affairs, InvaGen Pharmaceuticals (A Cipla Subsidiary), 550 S Research Place, Central Islip, 11730, USA*
[g]*KL Business School, Koneru Lakshmaiah Education Foundation, Vijayawada, Andhra Pradesh - 520 002, India*
[h]*Crescent School of Pharmacy, BS Abdur Rahman Crescent Institute of Science and Technology, Vandalur, Chennai 600048, India*

Use your device to scan and read the article online

Citation S. Ravindra Babu, V.R. Singamaneni, J. Mart E., P.V. Narasimha Raju, P. Erukulla, A. Manukonda, K.D. Hanumanthu, S. Prema, **Comprehensive Computational Exploration of Copper (II)–Benzimidazole Complexes as DNA Gyrase B Inhibitors: Integrated Molecular Modeling and Molecular Dynamics Approaches.** *J. Appl. Organomet. Chem.*, **2026**, *6*(2), 272-287.

https://doi.org/10.48309/JAOC.2026.560978.1364

Article info:
Submitted: 2025-11-09
Revised: 2025-12-25
Accepted: 2026-01-05
ID: JAOC-2511-1364

Keywords:
Copper (II) complexes, Benzimidazole, *Escherichia coli* DNA gyrase B, Molecular docking, Molecular dynamics simulation

ABSTRACT

The increasing prevalence of antimicrobial resistance, particularly among Gram-negative bacteria, emphasizes the critical need for new therapeutic approaches. This study investigated the inhibitory potential of four copper (II)-benzimidazole complexes against *Escherichia coli* DNA gyrase B, a key enzyme involved in bacterial DNA topology, which is a well-known target for antibacterial drug discovery. The stability and interaction behavior of the complexes were evaluated using a comprehensive computational pipeline that included molecular docking, MM/GBSA binding energy estimation, and 200 ns molecular dynamics simulations. Docking revealed that all the candidates fit comfortably within the ATP-binding site, with notable interactions involving residues such as Arg136, His55, Glu50, and Asp49. Dynamic analyses, such as RMSD, RMSF, radius of gyration, PCA, and free energy landscape mapping, revealed the conformational responses of the enzyme-ligand complexes. $Cu(C_{14}H_{12}BrN_3O_2)_2$ (compound **4**) consistently outperformed other compounds in terms of structural stability, conformational sampling restrictions, and thermodynamic favorability. This was further supported by MM/GBSA calculations, which revealed that compound **4** had a significantly lower binding free energy than those of the other complexes. Overall, this study identified compound **4** as a promising scaffold for further development as a DNA gyrase B inhibitor. These results highlight the importance of copper (II)-benzimidazole systems in antimicrobial drug design and provide a molecular foundation for future experimental and structural refinement efforts.

***Corresponding Authors: Joel Mart E.** (joelmart5@gmail.com), **S. Prema** (premspharm@gmail.com)*

Introduction

Development and high rate of spread of drug-resistant bacteria have emerged as significant health issues worldwide. Pathogenic bacteria, especially Gram-negative species such as *Escherichia coli*, *Klebsiella pneumoniae*, *Pseudomonas aeruginosa*, and *Acinetobacter baumannii*, have increasingly developed multidrug resistance (MDR). This increase in resistance is largely attributed to the unregulated use and overuse of antibiotics over the past several decades in both clinical and agricultural settings [1–4]. World health organization (WHO) provides a figure of approximately 1.27 million deaths caused by antimicrobial resistance (AMR) each year, and 4.95 million deaths caused by bacterial AMR in 2019 alone. It has been estimated that the number of deaths globally may increase by 10 million per year by 2050, which is greater than the increase in cancer-related deaths unless effective interventions are invented [5–7]. The present antibacterial treatments encounter the serious problems of limited activity against resistant bacterial strains, lack of target specificity, and the rapid ability of the bacterial defenses to adapt to the treatment. In particular, Gram-negative bacteria have an extra outer membrane and highly effective efflux pumps that make them inherently less susceptible to many drugs. In addition, the diminishing pipeline for new antibiotic development has intensified the urgency to explore alternative strategies. This includes investigating new chemical scaffolds and non-conventional antimicrobial approaches that may circumvent the existing resistance mechanisms [8–10]. DNA gyrase is a type II topoisomerase unique to bacteria, and is an important enzyme that introduces negative supercoils in DNA to allow replication and transcription. Its gyrase B (GyrB) subunit is essential for ATP hydrolysis, which is required for the passage of strands, and is therefore a proven and promising antibacterial antigen [11,12]. Blockage of GyrB interferes with DNA topology and results in the death of bacterial cells; therefore, blocking this enzyme is one of the best potential targets for designing antibacterial drugs. Nevertheless, the growing opposition to fluoroquinolone-historical gyrase inhibitors has reduced the clinical effectiveness of these drugs, and it is necessary to discover new drugs that can effectively interact with the active site of GyrB [12–14].

Recently, transition metal complexes have attracted great interest in medicinal chemistry because of their versatile coordination chemistry, distinct redox properties, and interactions with biological macromolecules. Copper (II) complexes, in particular, have demonstrated significant biological potential due to their redox activity, moderate toxicity, and ability to generate reactive oxygen species to increase their antimicrobial effects. The benzimidazole scaffold is a privileged pharmacophore with widely recognized biological actions, such as antibacterial, antifungal, and anticancer activities [15–18]. It is a multifunctional ligand that can bind metal ions via nitrogen donors, thereby enhancing the physicochemical stability and bioactivity of metal-based complexes. The integration of copper (II) ions with benzimidazole derivatives is a logical approach for the development of powerful DNA gyrase B inhibitors. The metal center allows positive electrostatic and coordination interactions in the GyrB ATP-binding pocket, while the benzimidazole moiety can improve π-π stacking and hydrogen bonding to significant residues. These hybrid complexes can be used to overcome traditional resistance mechanisms and offer novel directions for antibacterial development [19,20].

Batool *et al.* previously synthesized and characterized a series of copper (II)–benzimidazole complexes that exhibited significant antimicrobial potential [21]. Building upon their structural framework, the present study employed these reported copper (II)–benzimidazole complexes to computationally investigate their inhibitory potential against the DNA GyrB enzyme of *Escherichia coli*. The current work integrates molecular docking, MM-GBSA binding energy estimation, molecular dynamics (MD) simulations, and post-simulation analyses, such as principal component analysis (PCA) and free energy landscape analysis. These

combined approaches elucidate the stability, flexibility, and dynamic behavior of ligand–protein complexes. Through this comprehensive computational approach, this study aims to uncover the key molecular determinants governing the inhibitory mechanism of copper (II)–benzimidazole complexes, providing valuable insights for the rational design of next-generation antibacterial agents effective against resistant Gram-negative pathogens.

Materials and Methods

Molecular docking studies

The binding affinity and interaction pattern of copper (II) derivatives of substituted benzimidazoles (compounds **1**-**4**) were determined by molecular docking to the *Escherichia coli* DNA gyrase B enzyme. The crystal structure of the *Escherichia coli* DNA gyrase B complex with a benzothiazole-based inhibitor (PDB ID: 5L3J) was downloaded from the Protein Data Bank (PDB). Before docking, the protein structure was optimized in the Protein Preparation Wizard of Schrödinger Maestro (v2024-1) by assigning bond orders, including missing hydrogen atoms in the structure, eliminating crystallographic water molecules of the co-crystallized ligand beyond a distance of 5 Å, and optimizing bond protonation states at physiological pH (7.4). Energy minimization was then performed on the structure using the OPLS4 force field to eliminate steric clashes and maximize the geometry. The structures of the copper (II)-benzimidazole derivatives (**1**-**4**) were drawn using ChemDraw and minimized to three-dimensional structures using the LigPrep module. The Epik tool was used to create possible ionization states and tautomers at pH 7.0 ± 0.2. The coordination interactions between the central metal atom and the ligands were reconfigured in the workspace as coordination interactions by choosing the zero-order bonds to the metal option in the build menu. Partial atomic charges were calculated based on the OPLS4 force field, and all ligands were minimized prior to docking. The receptor grid was outlined in relation to the co-crystallized ligand-binding site of the GyrB subunit to be able to direct the target of the ATP-binding pocket with the highest accuracy. The resulting protein-ligand complexes were further studied using the Maestro pose viewer, which illustrated the hydrogen bonding interactions, π-π stacking interactions, and metal coordination interactions [22–24].

Molecular dynamics workflow

The structural stability and conformational behavior of top-ranked copper (II)-benzimidazole-GyrB complexes were simulated using Desmond (Schrödinger, 2024-1) to determine their molecular structure. Each complex was placed in an orthorhombic SPC water box with a 10 Å buffer zone, neutralized by including counter ions, and spiked with 0.15 M NaCl to make it similar to physiological conditions. The OPLS4 force field was parameterized, its energy was minimized, and the systems were equilibrated in the NPT ensemble (300 K, 1 bar) using the Nose-Hoover thermostat and Martyna-Tobias-Klein barostat. A production run of 200 ns was conducted at a 2fs integration step and recording of trajectories after every 100 ps. Post simulation analyses, such as root mean square deviation (RMSD), root mean square fluctuation (RMSF), hydrogen bonding, PCA, and free energy landscape (FEL), were performed to assess the stability of the complex and conformational dynamics [25,26].

Structural flexibility and energy profiling

PCA was used to acquire information about the overall motion and conformational flexibility of the proteins on a large scale during the simulation. This approach assisted in determining the prevailing motion patterns that characterize the dynamic behavior of DNA gyrase B-ligand complexes. To further assess the thermodynamic stability, FEL mapping was calculated, providing a pictorial representation of the most energetically favorable conformations and potential transition states. Conformational sampling with FEL analysis provided more in-depth insight into the

fluctuations of the complexes between the stable and metastable states. The trj_essential_dynamics utility of the Schrödinger package was employed to compute both PCA and FEL [27,28].

Post-dynamics binding energy assessment

The binding free energy of each protein–ligand complex was estimated using the Molecular Mechanics Generalized Born Surface Area (MM/GBSA) approach. Trajectories from the 0 to 200 ns molecular dynamics simulations were extracted and analyzed using the Prime module of the Schrödinger suite. The thermal_mmgbsa.py script was employed to calculate the average binding free energy across the simulation frames, providing a quantitative measure of ligand stability and affinity within the gyrB-binding pocket [29,30].

Results and Discussion

In the present study, four copper (II)–benzimidazole complexes previously synthesized and characterized by Batool *et al.* were selected for computational evaluation as potential DNA gyrase B inhibitors. The reported complexes were formed by coordinating Cu(II) ions with substituted benzimidazole ligands, yielding the following compositions: $[Cu(C_{15}H_{13}N_3O_4)_2]$ (**1**), $[Cu(C_{16}H_{16}N_2O_2)_2]$ (**2**), $[Cu(C_{15}H_{13}ClN_2O_2)_2]$ (**3**), and $[Cu(C_{14}H_{12}BrN_3O_2)_2]$ (**4**). According to the experimental findings of Batool *et al.*, these complexes displayed remarkable antibacterial activity against *Escherichia coli*, *methicillin-resistant Staphylococcus aureus* (MRSA), and *Acinetobacter baumannii*, exhibiting potent inhibitory effects and a minimum inhibitory concentration (MIC) of 25 µg/mL. Previous studies have established that benzimidazole derivatives can mimic the adenine moiety of ATP, enabling them to occupy the nucleotide-binding site and interfere with the enzyme's ATP hydrolytic activity, which is an essential step in DNA supercoiling and bacterial replication [31,32]. Based on these promising biological results, the current computational investigation was conducted to gain deeper molecular insights into their binding affinity, interaction mechanism, and dynamic stability within the active site of *Escherichia coli* DNA gyrase B. An integrated approach, which combines molecular docking, MM/GBSA free energy estimation, and MD simulations, was employed to rationalize the observed antibacterial activity and to explore the potential of these Cu (II)–benzimidazole complexes as promising scaffolds for antibacterial drug development.

Evaluation of docking outcomes

Molecular docking of the copper (II)-benzimidazole complexes (**1-4**) with *Escherichia coli* DNA gyrase B revealed different patterns of interactions and binding affinities in the ATP-binding pocket. Compound **1** $Cu(C_{15}H_{13}N_3O_4)_2$ had a docking score of-4.971 kcal/mol, with a binding affinity that was stable and moderately strong (**Table 1**). The complex created a hydrogen bond with the residue, and Arg136, and its terminal nitro group was ionically stimulated by residues Glu50 and Asp49, which are considered to be essential in the process of ATP coordination (**Figure 1**). These polar and electrostatic contacts help to anchor the compound appropriately within the active site, contributing to the positive docking energy. Compound **2**, $Cu(C_{16}H_{16}N_2O_2)_2$, showed a marginally higher docking score of -5.188 kcal/mol, indicating a better binding affinity than compound **1**. The van der Waals force stabilized the complex, although no direct hydrogen or ionic interactions were observed between the complex and the hydrophobic residues surrounding the nucleotide-binding cavity (**Figure 2**). Compound **3** $Cu(C_{15}H_{13}ClN_2O_2)_2$, however, had the lowest docking score (-3.874 kcal/mol), indicating the least binding among the four complexes. The interaction pattern showed that there was only a single hydrogen bond between the benzimidazole nitrogen and Asn46, and no other polar or ionic contacts stabilized the complex (**Figure 3**).

Table 1. Docking scores of Cu (II)–benzimidazole complexes with *Escherichia coli* DNA gyrase B (PDB ID: 5L3J)

Compound No.	Chemical compositions	Structure	Docking score
Compound **1**	$Cu(C_{15}H_{13}N_3O_4)_2$	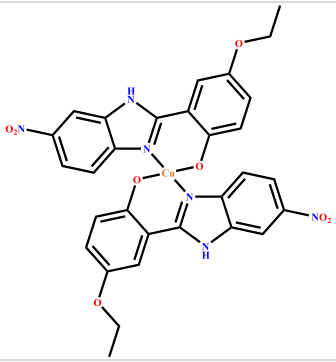	-4.971
Compound **2**	$Cu(C_{16}H_{16}N_2O_2)_2$	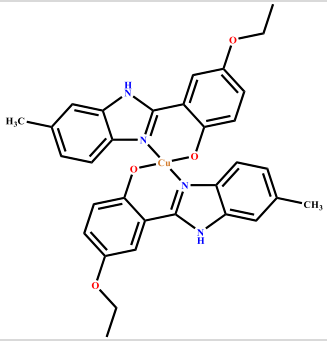	-5.188
Compound **3**	$Cu(C_{15}H_{13}ClN_2O_2)_2$	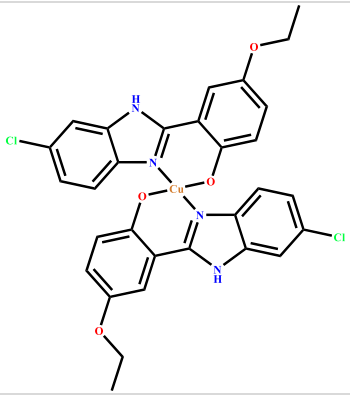	-3.874
Compound **4**	$Cu(C_{14}H_{12}BrN_3O_2)_2$	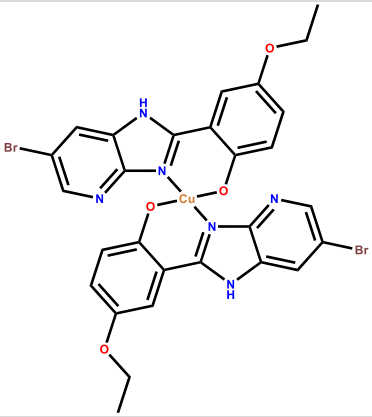	-5.236

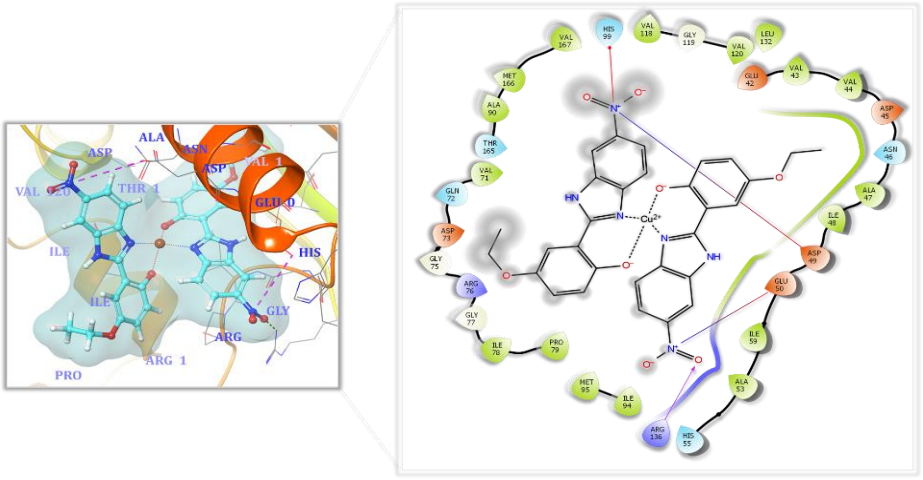

Figure 1. 2D and 3D predicted the binding modes of copper (II)–benzimidazole compound **1** within the active site of *Escherichia coli* DNA gyrase B (PDB ID: 5L3J)

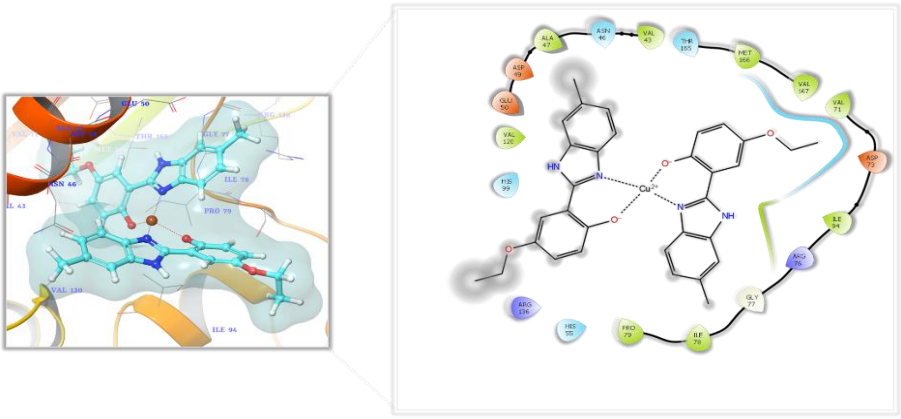

Figure 2. 2D and 3D predicted the binding modes of copper (II)–benzimidazole compound **2** within the active site of *Escherichia coli* DNA gyrase B (PDB ID: 5L3J)

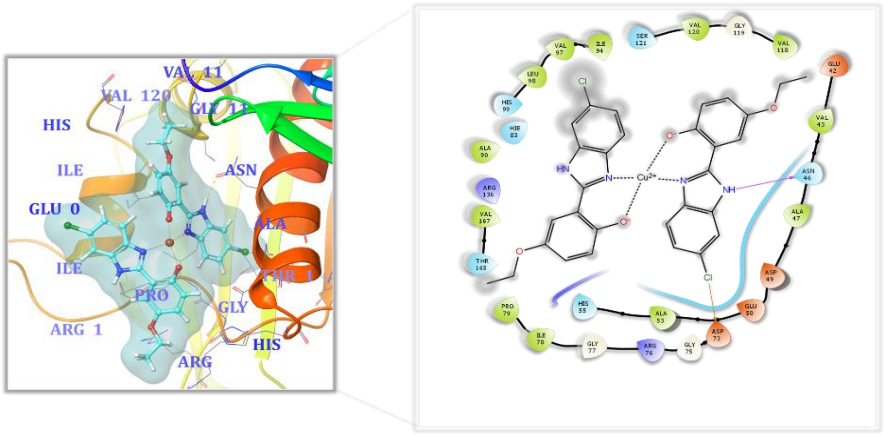

Figure 3. 2D and 3D predicted the binding modes of copper (II)–benzimidazole compound **3** within the active site of *Escherichia coli* DNA gyrase B (PDB ID: 5L3J)

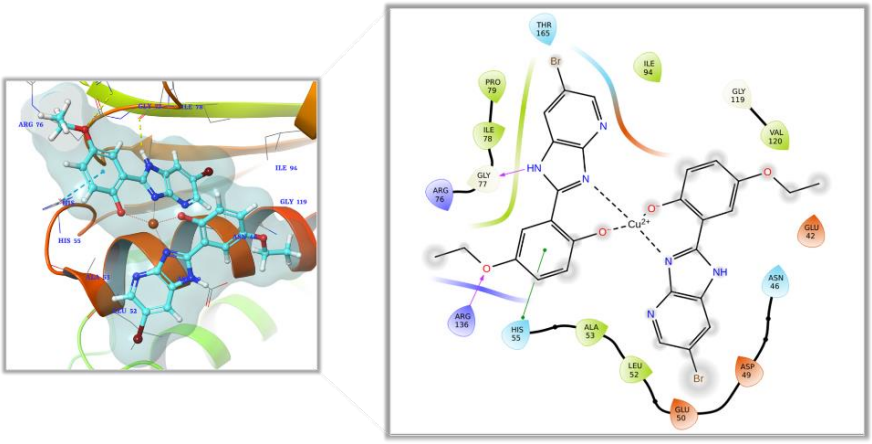

Figure 4. 2D and 3D predicted the binding modes of copper (II)–benzimidazole compound **4** within the active site of *Escherichia coli* DNA gyrase B (PDB ID: 5L3J)

The reduced affinity of the chloro substituent, which is less polarizable than bromine, might have contributed to the decreased electronic interaction, poor fit in the binding cavity, and reduced affinity. Conversely, compound **4** $Cu(C_{14}H_{12}BrN_3O_2)_2$ had the highest docking score (-5.236 kcal/mol), which implies that it has a potential binding interaction with DNA gyrase B. The complex formed a hydrogen bond between its terminal ethoxy group and Arg136, with its phenyl ring exhibiting a π-π stacking interaction with His55, resulting in both polar and hydrophobic stabilization in the ATP-binding region (**Figure 4**). These interactions are presumably reinforced by the increased electronic polarizability of the bromine atom, which explains its high docking energy. In general, the docking results showed that the binding affinity of compound **4** was higher than that of compounds 2, 1, and 3, making it the most promising inhibitor. Hydrogen bonding, ionic contacts, and aromatic stacking interactions with residues including Arg136, His55, Glu50, and Asp49 seem to be important for stabilizing the Cu (II)-benzimidazole complexes in the GyrB active site and suggest their potential as effective antibacterial targets for DNA gyrase B.

Molecular dynamics trajectory insights

To determine the binding stability and dynamics of the promising candidates, compounds **2** and **4**, 200-ns long molecular dynamics (MD) simulations with Desmond were conducted. These simulations were performed to observe the structural stability of the protein-ligand complexes and the conformational changes that occur during this time. The post-simulation analysis was carried out in detail and consisted of RMSD, RMSF, radius of gyration (RGyr), PCA, FEL, and MM/GBSA binding free energy calculations. The RMSD plot of the compound **2**-5L3J and compound **4**-5L3J complexes over 200 ns indicates that both systems undergo an initial structural change during the first 10-15 ns, where the RMSD increases rapidly from below 1.0 Å to approximately 2.0-2.5 Å. This implies that the protein-ligand environment relaxes once the simulation begins. Once this initial equilibration stage is completed, both complexes evolve into a relatively steady dynamic regime, although they still oscillate within a characteristic range over the course of the trajectory (**Figure 5**). Compound **2**-5L3J complex had more fluctuations in 2.5-4.0 Å with a maximum RMSD of 4.16 Å and a mean of 3.07 Å, indicating moderate flexibility of the protein in conformational changes with ligand binding. Amazingly, its RMSD is more likely to increase slowly after 120 ns, which suggests larger, but nevertheless controlled, rearrangements in the binding pocket. Conversely, the 4-5L3J complex (purple) stabilized after a little longer and had narrower fluctuations.

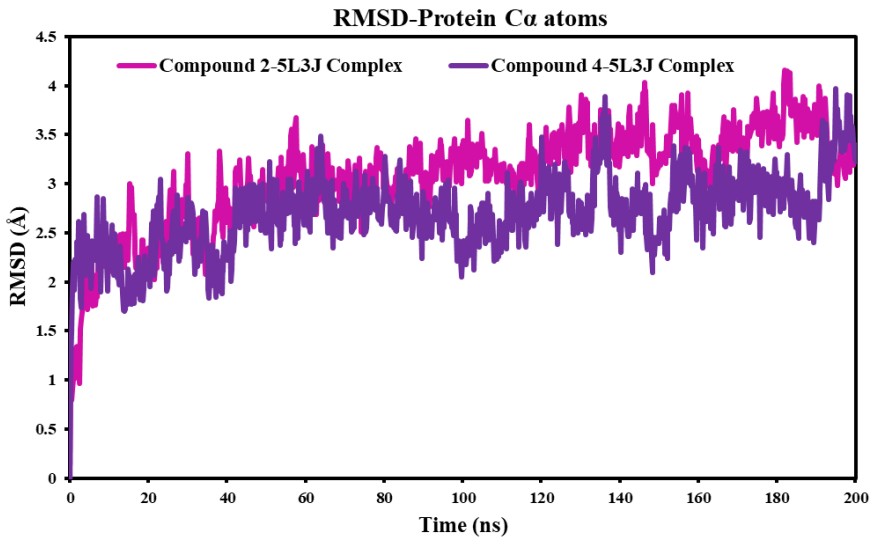

Figure 5. Time-dependent Cα-RMSD of the GyrB–compound **2** and GyrB–compound **4** complexes over 200 ns, showing overall structural stability and equilibration behavior of the protein–ligand systems

The RMSD values remained within the range of 2.2–3.5 Å, with a maximum peak of 3.97 Å and an average RMSD of 2.69 Å; the trajectory exhibited fewer abrupt shifts, particularly after 40 ns, indicating enhanced structural stability. This is because the protein-ligand complex was more stable and had a more consistent shape during the simulation. Both complexes were generally stable with acceptable RMSD values of over 200 ns. However, the compound **4** complex had a lower average RMSD and smaller amplitude of fluctuation, which suggests that it interacts with the DNA gyrase B active site more stably. This is in line with the higher binding affinity observed in docking experiments. RMSF analysis provided insights into the residue-level flexibility of DNA gyrase B in complex with compounds **2** and **4** over the 200 ns simulation. The compound **2**–5L3J complex had an average RMSF of 1.50 Å, with fluctuations of up to 6.59 Å (**Figure 6**). This means that some parts of the protein are moderately to highly flexible. Most of the residues that interact with the ligand, such as Val43(0.72 Å), Asn46(0.97 Å), Ala47(0.84 Å), Glu50(1.08 Å), Val71(0.58 Å), Asp73(0.74 Å), Arg76(1.10 Å), Gly77(1.01 Å), Ile78(1.07 Å), Pro79 (1.47 Å), Ile82 (2.63 Å), Ala90(2.79 Å), Ala91(1.68 Å), Val93(1.62 Å), Ile94(1.56 Å), Met95 (1.21 Å), His99(2.35 Å), Val118(2.04 Å), Val120(1.14 Å), Ser121(1.10 Å), Leu132 (0.73 Å), Thr165(0.65 Å), and Val167(0.72 Å), showed fluctuations below ~1.5 Å, which means they stayed in contact with the ligand throughout the simulation. The compound **4**–5L3J complex, on the other hand, had a lower average RMSF of 1.26 Å and a lower maximum fluctuation of 4.96 Å, indicating that it was more structurally stable. Key interacting residues, such as Glu42(0.81 Å), Val43(0.75 Å), Asn46(0.97 Å), Ala47(0.83 Å), Asp49(1.04 Å), Glu50(1.03 Å), Leu52(1.41 Å), Ala53(1.56 Å), His55(1.21 Å), Asp73(0.75 Å), Arg76(1.16 Å), Gly77(1.01 Å), Ile78(1.17 Å), Pro79(1.39 Å), Ile94(1.19 Å), His99(1.82 Å), Val118(1.40 Å), Gly119(1.17 Å), Val120(0.79 Å), Ser121(0.70 Å), Arg136(1.20 Å), Pro328(1.25 Å), and Asp329(1.35 Å), generally showed fluctuations below 1.5 Å. Arg136 and His55, which are important anchoring residues that form hydrogen bonds and π–π interactions with compound **4**, remained stable throughout the trajectory. This finding supports the robust binding stability observed in the docking data. Overall, compound **4** maintained tighter and more consistent interactions with the active-site residues compared with compound **2**, supporting its lower RMSD, lower RMSF, and superior docking score. The profile of the RGyr of both complexes shows that the general

compactness of DNA gyrase B was still very much maintained throughout the 200 ns simulation of the run. The average RGyr value in both systems is very similar (compound **2**: 26.76 Å; compound **4**: 26.93 Å) indicating that there is no significant difference in the global folding state of the protein between the two complexes (**Figure 7**). Nevertheless, the maximal RGyr is different: compound **2** has a higher peak (32.73 Å) in comparison to compound 4 (30.59 Å). This means that compound **2** produces some medium-sized protein expansions (transient loosening or breathing motions), whereas compound **4** maintains a steadier compactness along the trajectory.

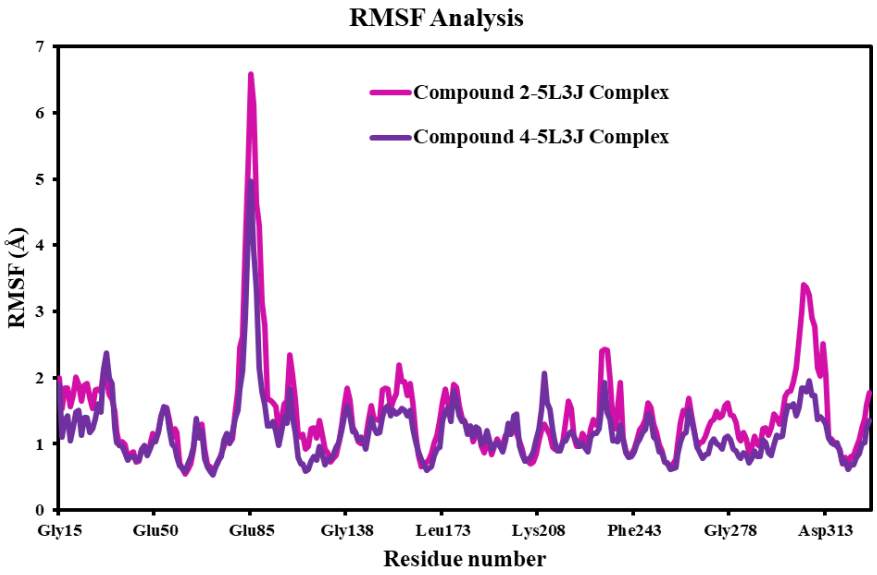

Figure 6. Per-residue RMSF values for the compound **2**–5L3J and compound **4**–5L3J complexes, highlighting flexible regions and the stability of key ligand-interacting residues

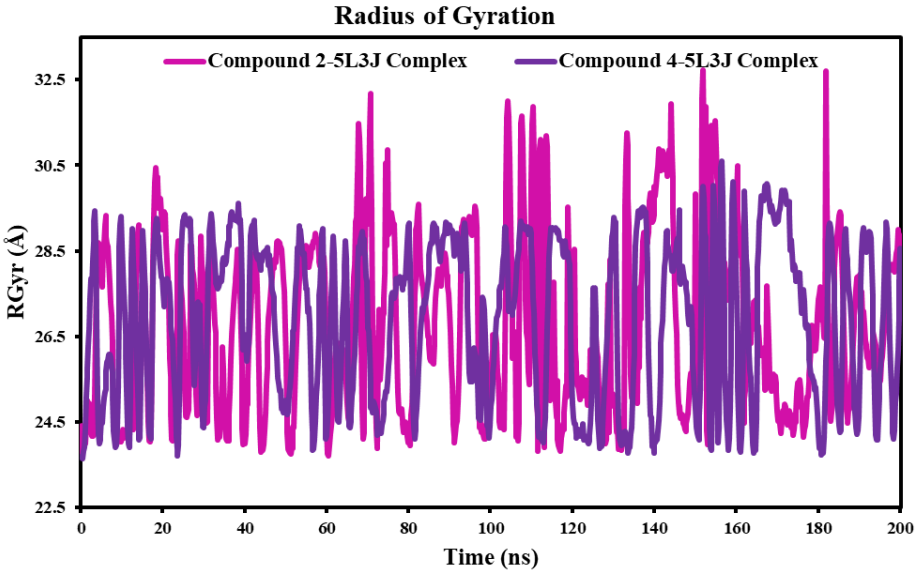

Figure 7. Radius of gyration variations of the compound **2**–5L3J complex and compound **4**–5L3J complex, indicating overall protein compactness and maintenance of global fold during the trajectory

Structural dynamics and energetic features

Principal component analysis

PCA analysis helped to understand the collective movements of the compounds **2**-5L3J and 4-5L3J complexes on a large scale over the 200 ns of simulation. As depicted in the PCA scatter plot (**Figure 8**), both complexes covered large, but partially overlapping, conformational spaces along PC1 and PC2, which means that the general flexibility pattern of DNA gyrase B was maintained in both systems. Nevertheless, the compound **2**-5L3J complex had a more diffuse distribution of points, especially at the positive and negative ends of PC1, indicating that the protein sample had a wider range of conformational states when occupied by compound **2**. In contrast, the 4-5L3J complexes had a less extended pattern of clustering, which is indicative of more restricted movement and a more reliable conformational ensemble. This was also observed in variance plots. In both complexes, the initial few major components control global motion, but the magnitude varies. PC1 contributes approximately 23-25% of the motion in the compound **2**-5L3J complex, with increasingly smaller contributions from PC2 and PC3, which implies that the first modes represent significant flexibilities (**Figure 9**). The compound **4**-5L3J complex, on the other hand, has a significantly larger contribution of PC1 (around 27-28%), but with an even steeper drop in the following components, implying that the movement is concentrated on a few dominant modes with the remaining space of conformational space being reasonably stable. In general, PCA showed that compound **4** was more likely to induce compact and energetically preferred motions, which was observed in its decreased RMSD and RMSF, while compound **2** provided larger conformational sampling as it is more flexible in terms of dynamics. These results support the docking and MD stability studies, which indicate that compound 4 reacts more strongly and stabilizes the GyrB active site better than compound **2**.

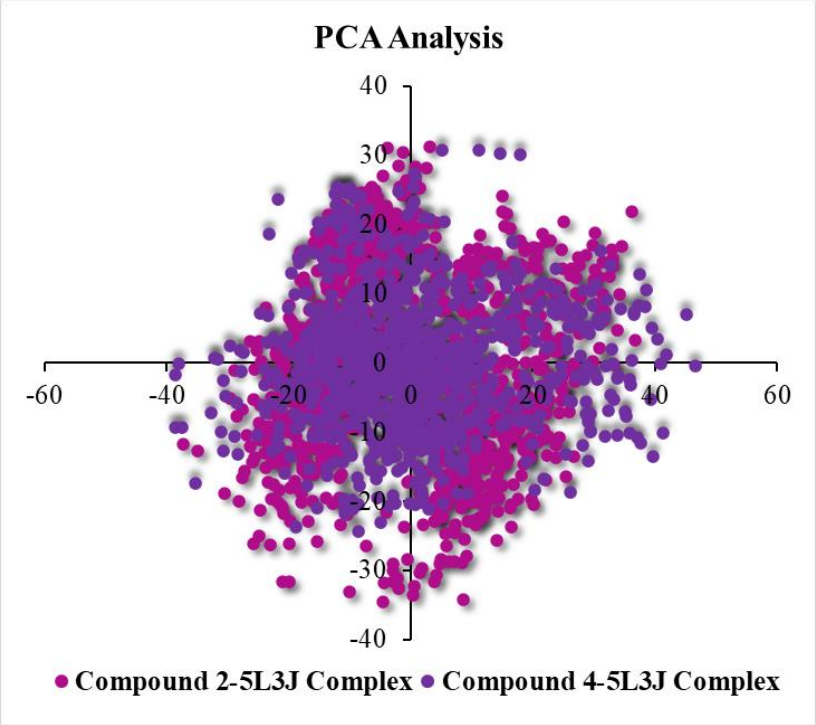

Figure 8. PCA scatter plot of DNA gyrase B complexes with compounds **2** and **4**

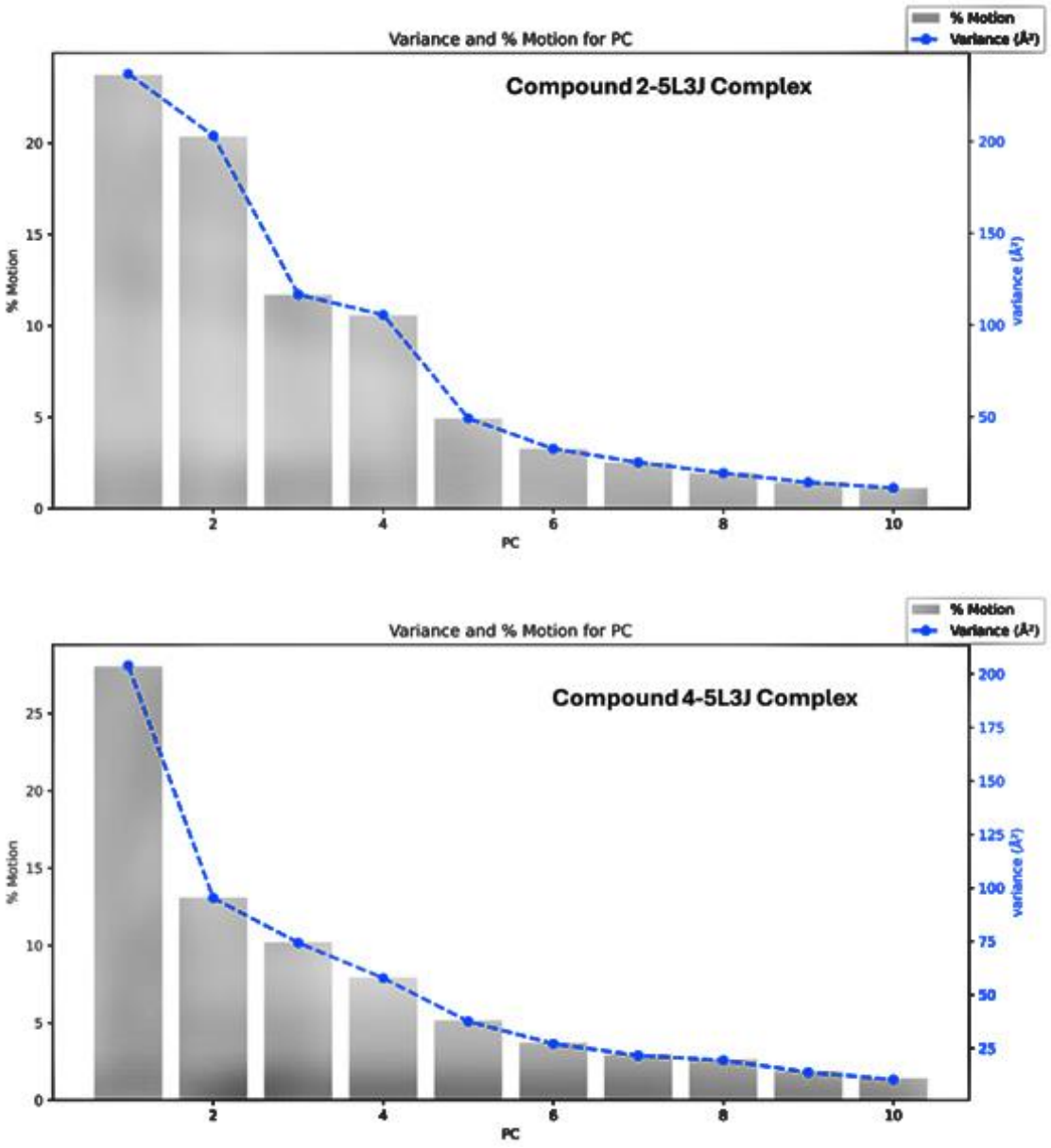

Figure 9. Variance contribution and percentage motion of principal components for compounds **2**–5L3J and **4**–5L3J complexes

Free energy landscape (FEL) analysis

FEL analysis provided a more detailed understanding of the thermodynamically favored conformations sampled by the compounds **2**-5L3J and 4-5L3J complexes during the 200 ns simulation. Both surfaces had several shallow basins, indicating that DNA gyrase B continuously underwent microstate changes while maintaining a generally stable fold. However, the distribution and depth of these basins vary between the two systems. The compound **2**-5L3J complex displayed the lowest energy state at frame 576, which had a radius of gyration of 29.04 Å, RMSD of 2.77 Å, and minimum free energy of 2.589 kcal/mol (**Figure 10**). This implies that the complex stabilizes a relatively expanded but energetically favorable conformation.

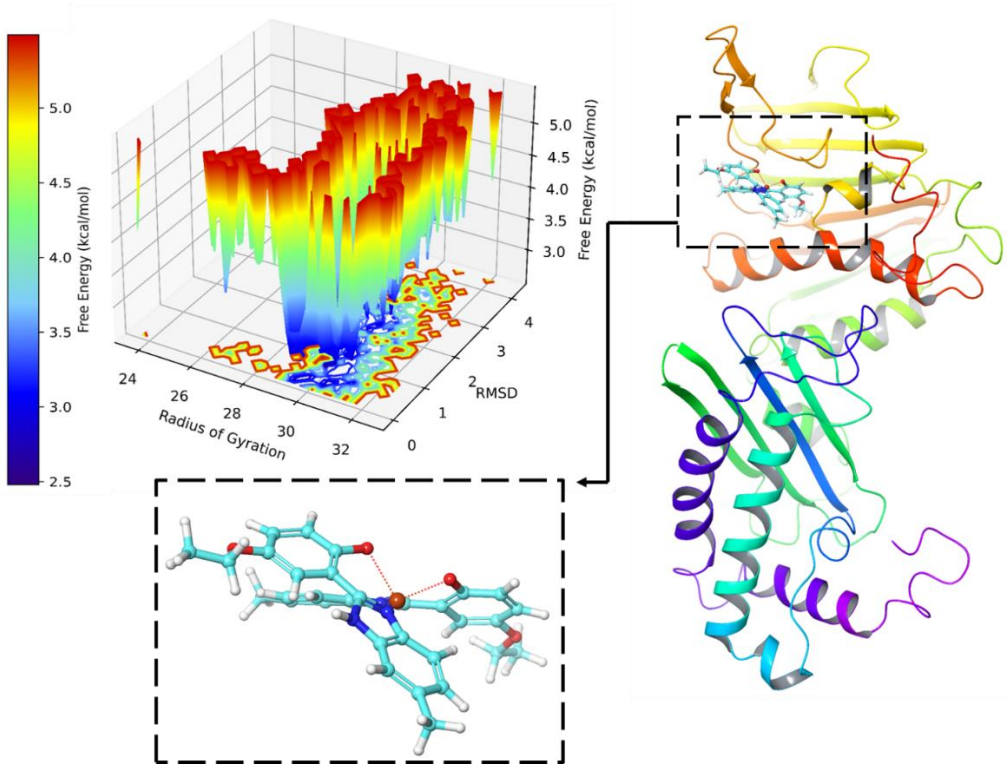

Figure 10. Free energy landscape of the DNA Gyrase B complexes with compound **2**

Conversely, the compound **4**-5L3J complex had a global minimum at frame 604, where the conformation of the protein was smaller with a radius of gyration of 26.16 Å, an RMSD of 3.20 Å and a free energy minimum of 2.504 kcal/mol compared to any other frame of the two systems (**Figure 11**). This more compact PCA clustering and smaller RMSF values of the compound **4**-5L3J complex are indicated by the observed deeper and more concentrated energy basin, which suggests a more limited conformational space and higher thermodynamic stability. On the other hand, wider sampling of low-energy regions of the compound **2**-5L3J landscape suggests increased conformational flexibility and coverage of several microstates (**Table 2**). A combination of these findings implies that compound **4** holds DNA Gyrase B in a more energetically conducive and structurally compacted ensemble but covers a broader conformational space with stabilized binding using compound **2**. The FEL results thus support the RMSD, RMSF, and PCA results, which indicate compound **4** as a more dynamically stable and tightly bound inhibitor candidate.

MM/GBSA-based energy profiling

MM/GBSA analysis provided quantitative information about the energetic contributions that govern compounds **2** and 4 binding to the DNA gyrase B active site. Compound **4** (-41.598 ± 5.294 kcal/mol) binds significantly more strongly than compound **2** (-25.248 ± 5.532 kcal/mol), indicating markedly higher thermodynamic favorability. Compound **4** had a higher electrostatic component (-79.851 ± 6.278 kcal/mol) than compound **2** (-59.570 ± 5.696 kcal/mol), which contributed significantly to the difference. This demonstrates that compound **4** has stronger ionic and polar interactions within the ATP-binding pocket, which is consistent with its stable hydrogen-bonding network and interactions with residues such as Arg136 and Asp49.

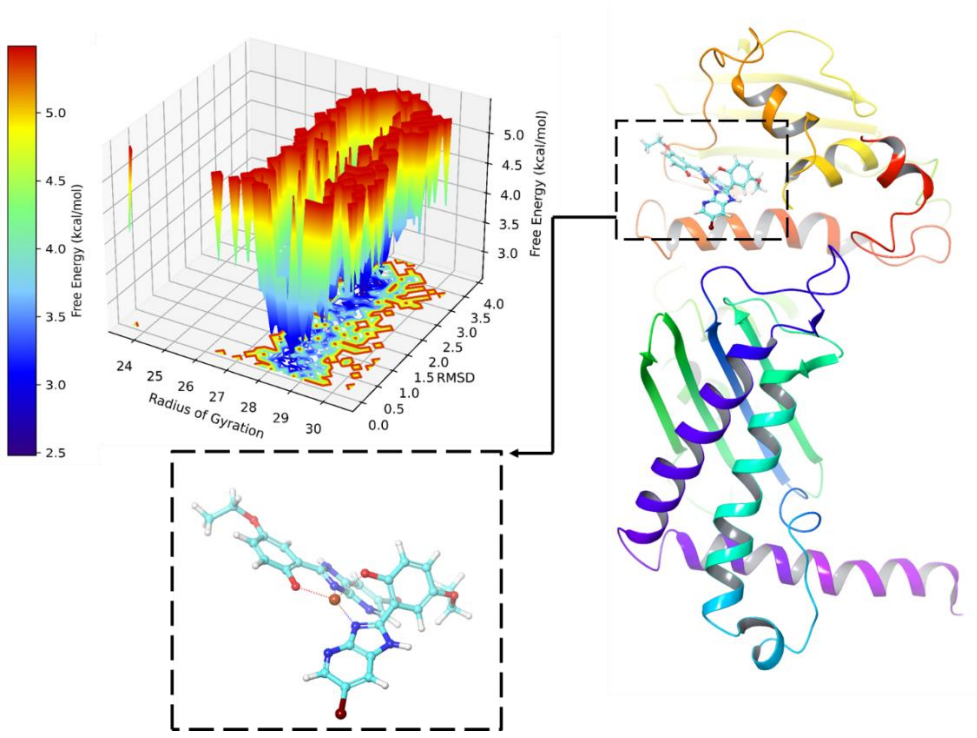

Figure 11. Free energy landscape of the DNA gyrase B complexes with compound **4**

Table 2. MM/GBSA binding free energy components of the compounds **2**–5L3J and **4**–5L3J complexes calculated over 1000 frames extracted from the 200 ns MD trajectories

Energy component	Compound 2–5L3J	Compound 4–5L3J
ΔG_{bind}	-25.248 ± 5.532	-41.598 ± 5.294
$\Delta G_{bindCoul}$	-59.570 ± 5.696	-79.851 ± 6.278
$\Delta G_{bindHbond}$	-0.184 ± 0.198	-0.511 ± 0.266
$\Delta G_{bindLip}$	-20.780 ± 2.078	-14.528 ± 1.155
$\Delta G_{bindsol\_GB}$	109.618 ± 9.175	106.539 ± 5.065
$\Delta G_{bindvdw}$	-55.095 ± 6.189	-52.185 ± 3.701

Compound **4** (-52.185 ± 3.701 kcal/mol) and compound **2** (-55.095 ± 6.189 kcal/mol) were stabilized by van der Waals interactions ($\Delta G_{bindvdw}$). Compound 2 had a stronger hydrophobic contribution ($\Delta G_{bindLip}$) (-20.780 ± 2.078 kcal/mol) than compound **4** (-14.528 ± 1.155 kcal/mol), but this advantage was outweighed by compound **4**'s significantly higher electrostatic gains. Both complexes had modest hydrogen-bonding energies ($\Delta G_{bindHbond}$), but compound **4** had a lower $\Delta G_{bindHbond}$ (-0.511 ± 0.266 kcal/mol), indicating more persistent H-bond interactions during the MD trajectory (**Table 2**). The polar solvation penalty ($\Delta G_{bindsol\_GB}$) hindered the binding of both ligands, but compound **4** had a slightly smaller effect (106.539 ± 5.065 kcal/mol) than compound **2** (109.618 ± 9.175 kcal/mol), resulting in a higher net binding affinity. Overall, the MM/GBSA results clearly show that compound **4** achieves stronger binding through a synergistic contribution of improved electrostatic interactions, favorable van der Waals contacts, and a reduced solvation penalty, which is consistent with its superior RMSD, RMSF, PCA, and FEL stability profiles. Compound **2**, while moderately stabilizing, exhibited a weaker electrostatic and solvation balance, which explains its lower total binding energy.

Conclusion

In conclusion, this study presents a comprehensive computational evaluation of four copper (II)–benzimidazole complexes to determine their potential as inhibitors of *Escherichia coli* DNA gyrase B. Molecular docking showed that all complexes bind well to the ATP-binding pocket, with compound **4** exhibiting the highest affinity due to stable hydrogen bonding and π–π interactions with key residues such as Arg136 and His55. Molecular dynamics simulations confirmed these findings, with all complexes maintaining stable interactions over 200 ns trajectories; however, compound **4** consistently demonstrated superior structural stability, as shown by its lower RMSD and RMSF values and a more compact radius of gyration. PCA and FEL analyses further indicated that compound **4** stabilizes GyrB in fewer and more energetically favorable conformational basins, whereas compound **2** samples a broader range of microstates. These results align with MM/GBSA calculations, which showed a significantly lower binding free energy for compound **4** (–41.60 kcal/mol) compared to compound **2** (–25.25 kcal/mol), reflecting its stronger electrostatic and van der Waals contributions within the active site. Overall, the combined computational evidence clearly identifies compound **4** as the most promising inhibitor among the tested complexes. These findings provide important molecular insights that support future experimental evaluations of copper (II)–benzimidazole scaffolds through enzymatic assays and antibacterial testing.

Acknowledgments

None.

Conflicts of Interest

Authors are declared that there no conflict of interest exists.

ORCID

Sajja Ravindra Babu
https://orcid.org/0000-0002-0633-1551

Venkata Ramana Singamaneni
https://orcid.org/0009-0006-4328-8253

Joel Mart E.
https://orcid.org/0009-0000-9560-674X

Pericharla Venkata Narasimha Raju
https://orcid.org/0009-0003-2259-6693

Phanindra Erukulla
https://orcid.org/0009-0001-2900-2881

Ajay Manukonda
https://orcid.org/0009-0000-9896-4796

Kanaka Durga Hanumanthu
https://orcid.org/0009-0005-8402-410X

S. Prema
https://orcid.org/0000-0002-3108-8979

References

[1] Murray, C.J., Ikuta, K.S., Sharara, F., Swetschinski, L., Aguilar, G.R., Gray, A., Han, C., Bisignano, C., Rao, P., Wool, E. Global burden of bacterial antimicrobial resistance in 2019: A systematic analysis. *The Lancet*, **2022**, 399(10325), 629-655.
[2] Ranjbar, R., Alam, M. Antimicrobial resistance collaborators (2022). Global burden of bacterial antimicrobial resistance in 2019: A systematic analysis. *Evidence-Based Nursing*, **2023**.
[3] Gómez-Ríos, D., Ramírez-Malule, H. Bibliometric analysis of recent research on multidrug and antibiotics resistance (2017–2018). *Journal of Applied Pharmaceutical Science*, **2019**, 9(5), 112-116.
[4] Palacios, O.A., Adame-Gallegos, J.R., Rivera-Chavira, B.E., Nevarez-Moorillon, G.V. Antibiotics, multidrug-resistant bacteria, and antibiotic resistance genes: Indicators of contamination in mangroves? *Antibiotics*, **2021**, 10(9), 1103.
[5] Ahmed, S.M., Naher, N., Tune, S.N.B.K., Islam, B.Z. The implementation of national action plan (nap) on antimicrobial resistance (amr) in bangladesh: Challenges and lessons learned from a cross-sectional qualitative study. *Antibiotics*, **2022**, 11(5), 690.
[6] Centers for Disease Control and Prevention (CDC). Antibiotic resistance threats report 2019. CDC, **2019**.
[7] Konwar, A.N., Hazarika, S.N., Bharadwaj, P., Thakur, D. Emerging non-traditional approaches to

combat antibiotic resistance. *Current Microbiology*, **2022**, 79(11), 330.
[8] Maher, C., Hassan, K.A. The Gram-negative permeability barrier: Tipping the balance of the in and the out. *MBio*, **2023**, 14(6), e01205-01223.
[9] Aghapour, Z., Gholizadeh, P., Ganbarov, K., Bialvaei, A.Z., Mahmood, S.S., Tanomand, A., Yousefi, M., Asgharzadeh, M., Yousefi, B., Kafil, H.S. Molecular mechanisms related to colistin resistance in enterobacteriaceae. *Infection and Drug Resistance*, **2019**, 965-975.
[10] Breijyeh, Z., Jubeh, B., Karaman, R. Resistance of Gram-negative bacteria to current antibacterial agents and approaches to resolve it. *Molecules*, **2020**, 25(6), 1340.
[11] Pantel, A., Petrella, S., Veziris, N., Brossier, F., Bastian, S., Jarlier, V., Mayer, C., Aubry, A. Extending the definition of the gyrb quinolone resistance-determining region in mycobacterium tuberculosis DNA gyrase for assessing fluoroquinolone resistance in m. Tuberculosis. *Antimicrobial Agents and Chemotherapy*, **2012**, 56(4), 1990-1996.
[12] Locher, C.P., Jones, S.M., Hanzelka, B.L., Perola, E., Shoen, C.M., Cynamon, M.H., Ngwane, A.H., Wiid, I.J., Van Helden, P.D., Betoudji, F. A novel inhibitor of gyrase b is a potent drug candidate for treatment of tuberculosis and nontuberculosis mycobacterial infections. *Antimicrobial Agents and Chemotherapy*, **2015**, 59(3), 1455-1465.
[13] Collin, F., Karkare, S., Maxwell, A. Exploiting bacterial DNA gyrase as a drug target: Current state and perspectives. *Applied Microbiology and Biotechnology*, **2011**, 92(3), 479-497.
[14] Zhang, J., Yang, Q., Romero, J.A.C., Cross, J., Wang, B., Poutsiaka, K.M., Epie, F., Bevan, D., Wu, Y., Moy, T. Discovery of indazole derivatives as a novel class of bacterial gyrase b inhibitors. *ACS Medicinal Chemistry Letters*, **2015**, 6(10), 1080-1085.
[15] Abdou, A., Khalaf, M.M., Abd El-Lateef, H.M. Synthesis and characterization of octahedral ni (ii) and cu (ii) complexes with imidazole-based ligands: Structural, dft, and molecular docking, enhanced antimicrobial, and anti-inflammatory activity. *Applied Organometallic Chemistry*, **2025**, 39(5), e70158.
[16] Ngece, K., Khwaza, V., Paca, A.M., Aderibigbe, B.A. The antimicrobial efficacy of copper complexes: A review. *Antibiotics*, **2025**, 14(5), 516.
[17] Rogalewicz, B., Czylkowska, A. Recent advances in the discovery of copper (ii) complexes as potential anticancer drugs. *European Journal of Medicinal Chemistry*, **2025**, 117702.
[18] Saha, A., Debnath, A., Chettri, M., Mahato, R.K., Das, D., Sarkar, D., Chaurasia, R., Bhattacharyya, S., Mukherjee, M., Biswas, B. Benzimidazole-coordinated copper (ii) complexes as effectual chemotherapeutics against malignancy. *ACS Omega*, **2025**, 10(31), 34399-34413.
[19] Kamoon, R.A., Talib, A.B., Sadiq, Z.A., Abdulhadi, S.L. Importance of coordination chemistry in anticancer, antimicrobial, and antioxidant therapy: A review. *Journal of Chemical Reviews*, **2025**, 7(1),1–24.
[20] Adhikari, S., Nath, P., Das, A., Datta, A., Baildya, N., Duttaroy, A.K., Pathak, S. A review on metal complexes and its anti-cancer activities: Recent updates from in vivo studies. *Biomedicine & Pharmacotherapy*, **2024**, 171, 116211.
[21] Batool, S., Zafar, A., Rashid, Z., Yousuf, S., Naz, S., Fatima, R., Haq, I., Waseem, A. Copper (ii) derivatives of substituted benzimidazoles: Synthesis, structural, computational, and biological studies. *Journal of Molecular Structure*, **2025**, 144048.
[22] Jadhav, S., Dighe, P. In vitro evaluation, and molecular docking studies of novel pyrazoline derivatives as promising bioactive molecules. *Journal of Pharmaceutical Sciences and Computational Chemistry*, **2025**, 1(3), 190-209.
[23] Siddiqui, F., Makhloufi, R., Salah, M.E.-S., Mohamed, E., Hojjati, M. Computational exploration of quinine and mefloquine as potential anti-malarial agents. *Journal of Pharmaceutical Sciences and Computational Chemistry*, **2025**, 1(2), 106-115.
[24] Tamboli, A., Tayade, S. In-depth investigation of berberine and tropane through computational screening as possible dpp-iv inhibitors for the treatment of t2dm. *Journal of Pharmaceutical Sciences and Computational Chemistry*, **2025**, 1(1), 1-11.
[25] Saiyad, A.H., Godhani, D.R., Mehta, U.P., Parmar, K.P., Mehta, J.P., Patel, H.M., Ahmad, I. Synthesis, antimicrobial activity, molecular docking and md simulation studies, in silico adme investigations and thermo-acoustic studies of heterocyclic dihydropyrimidine substituted 1, 3, 4-thiadiazole scaffolds. *Journal of Molecular Structure*, **2025**, 1321, 140083.
[26] Muslim, R.F., Guma, M.A., Mahmood, A.A.R., Ahmad, I., Hirad, A.H., Patel, H. Synthesis, characterization, molecular modeling studies and bioactivity of a novel bicyclic compound of δ-lactam with oxazepine ring containing sulphur substitute using an economic method. *Journal of Computational Biophysics and Chemistry*, **2025**, 24(06), 733-750.
[27] Ahmad, I., Patel, H. Mechanistic insights into the allosteric inhibition of egfr by dibenzodiazepinone ddc4002: A molecular dynamics, binding free energy, conformational motions and thermodynamic landscape approach. *In Silico Research in Biomedicine*, **2025**, 100048.

[28] Boulaamane, Y., Touati, I., Qamar, I., Ahmad, I., Patel, H., Chandra, A., Britel, M.R., Maurady, A. In silico discovery of dual ligands targeting mao-b and aa2ar from african natural products using pharmacophore modelling, molecular docking, and molecular dynamics simulations. *Chemistry Africa*, **2024**, 7(8), 4337-4359.
[29] Amadei, A., Linssen, A.B., Berendsen, H.J. Essential dynamics of proteins. *Proteins: Structure, Function, and Bioinformatics*, **1993**, 17(4), 412-425.
[30] Elsaman, T., Ahmad, I., Eltayib, E.M., Suliman Mohamed, M., Yusuf, O., Saeed, M., Patel, H., Mohamed, M.A. Flavonostilbenes natural hybrids from rhamnoneuron balansae as potential antitumors targeting aldh1a1: Molecular docking, admet, mm-gbsa calculations and molecular dynamics studies. *Journal of Biomolecular Structure and Dynamics*, **2024**, 42(6), 3249-3266.
[31] Mañozca-Dosman, I.V., Aragón-Muriel, A., Polo-Cerón, D. Antibacterial activity of metal complexes of cu (ii) and ni (ii) with the ligand 2-(phenylsubstituted) benzimidazole. *Scientia Pharmaceutica*, **2025**, 93(2), 22.
[32] Charifson, P.S., Grillot, A.-L., Grossman, T.H., Parsons, J.D., Badia, M., Bellon, S., Deininger, D.D., Drumm, J.E., Gross, C.H., LeTiran, A. Novel dual-targeting benzimidazole urea inhibitors of DNA gyrase and topoisomerase iv possessing potent antibacterial activity: Intelligent design and evolution through the judicious use of structure-guided design and stucture–activity relationships. *Journal of Medicinal Chemistry*, **2008**, 51(17), 5243-5263.